

## Evidence of Decay of Flux Ratio of Fe to Fe–Ni Line Features with Electron Temperature in Solar Flares

Rajmal Jain<sup>1</sup>, Malini Aggarwal<sup>2</sup> & Raghunandan Sharma<sup>1</sup>

<sup>1</sup>Physical Research Laboratory, Navrangpura, Ahmedabad 380 009, India.

<sup>2</sup>Solar and Space Weather Group, Korea Astronomy and Space Science Institute, Daejeon, Republic of Korea.

Received 2009 September 7; Accepted 2010 August 18

**Abstract.** We report observational evidence of the decay of the flux ratio of Fe to Fe–Ni line features as a function of plasma electron temperature in solar flares in comparison to that theoretically predicted by Phillips (2004). We present the study of spectral analysis of 14 flares observed by the Solar X-ray Spectrometer (SOXS) – Low Energy Detector (SLD) payload. The SLD payload employs the state-of-the-art solid state detectors, viz., Si PIN and Cadmium-Zinc-Telluride (CZT) devices. The sub-keV energy resolution of Si PIN detector allows us to study the Fe-line and Fe–Ni line features appearing at 6.7 and 8 keV, respectively, in greater detail. In order to best-fit the whole spectrum at one time in the desired energy range between 4 and 25 keV we considered Gaussian-line, the multi-thermal power-law and broken power-law functions. We found that the flux ratio of Fe to Fe–Ni line features decays with flare electron temperature by the asymptotic form of polynomial of inverse third order. The relative flux ratio is  $\sim 30$  at temperature 12 MK which drops to half,  $\sim 15$  at 20 MK, and at further higher temperatures it decreases smoothly reaching to  $\sim 8$  at  $\sim 50$  MK. The flux ratio, however, at a given flare plasma temperature, and its decrease with temperature is significantly lower than that predicted theoretically. We propose that the difference may be due to the consideration of higher densities of Fe and Fe–Ni lines in the theoretical model of Phillips (2004). We suggest revising the Fe and Fe–Ni line densities in the corona. The decay of flux ratio explains the variation of equivalent width and peak energy of these line features with temperature.

*Key words.* Sun: flares, corona—X-rays.

### 1. Introduction

The X-ray energy spectrum from a typical large solar flare is dominated by soft X-ray line and thermal (free–free) bremsstrahlung emission at  $\varepsilon \approx 1\text{--}20$  keV, and collisional bremsstrahlung of non-thermal electrons at  $\varepsilon \approx 20\text{--}1000$  keV (Jain *et al.* 2000a, 2000b, 2005; Dennis *et al.* 2005). The 1–10 keV spectrum contains emission lines of highly ionized Ca, Fe, and Ni atoms. The Fe-line complex at  $\sim 6.7$  keV is mostly due to

the  $1s-2p$  transitions in He-like and H-like iron, Fe XXV and Fe XXVI, respectively, with associated satellite lines. The weaker Fe–Ni line feature at  $\sim 8$  keV made up of emission from He-like nickel and more highly excited Fe XXV ions is also evident in the more intense flares (Phillips 2004; Phillips *et al.* 2004).

The detailed investigation by Jain *et al.* (2006b) of X-ray spectra of M-class flares observed by Si detector of SLD/SOXS mission (Jain *et al.* 2000a, 2000b, 2005, 2006a) showed that peak energy and equivalent width ( $w$ ) of Fe-line feature vary as a function of temperature of flare plasma. Further, they also showed that the whole energy spectrum of 4–20 keV cannot be fitted with single temperature approximation. They used two temperatures to obtain the best fit for line emission and continuum. The equivalent width of the Fe-line feature was observed to exceed the theoretical one in the temperature range of  $\approx 20-60$  MK, which could indicate multi-thermal flare plasma or higher iron flux. The ratio of the 6.7 keV Fe to the 8.0 keV Fe–Ni line fluxes is therefore expected to decrease progressively with higher plasma temperature. Phillips (2004) calculated the intensity ratio from Chianti but adding the intensity of satellites to the Fe XXV  $1s^2-1s^3p$  line that are omitted from Chianti. He predicted that the intensity ratio decreases by almost a factor of 2 from 20–30 MK, but at higher temperatures it decreases much more slowly. The critical temperatures for the formation of Fe and Fe–Ni line features were theoretically estimated by Phillips (2004) to be 10 and 15 MK, respectively. Jain *et al.* (2006b) found the signatures of Fe-line and Fe–Ni-line features to be sometimes even below 10 and 12 MK, respectively. However, measurement of the ratio of flux of Fe to Fe–Ni line features requires unambiguous identification of these features, which is possible when the detector reveals sub-keV spectral resolution. The high sensitivity and sub-keV (0.8 keV) energy resolution of Si PIN detector of the SOXS mission (Jain *et al.* 2000a, 2000b, 2005, 2006a) allows measuring of the intensity and mean energy of the Fe and Fe–Ni line features as a function of time in all classes of flares at approximately 6.7 and 8 keV, respectively (Jain *et al.* 2005, 2006b). Therefore, the purpose of this paper is to measure the flux ratio of Fe to Fe–Ni line features as a function of temperature in various M-class flares using the high sensitivity and sub-keV energy resolution capabilities of Si PIN detector of SLD/SOXS mission, and to compare the results with that theoretically predicted by Phillips (2004). In section 2, we describe observations and analysis techniques. Results and discussions are presented in section 3, and the paper is concluded in section 4.

## 2. Observations and analysis

### 2.1 Instrumentation

The SOXS (Jain *et al.* 2000a, 2000b, 2005, 2006a, 2008) aims to study the high energy and temporal resolution X-ray spectra from solar flares. The SOXS Low Energy Detector (SLD) payload is comprised of two semiconductor devices, viz., Silicon PIN detector (area  $11.56 \text{ mm}^2$ ) for 4–25 keV and Cadmium-Zinc-Telluride (CZT) detector (area  $25 \text{ mm}^2$ ) for 4–56 keV energy range. These state-of-the-art solid state detectors operate at near-room temperature, i.e., at  $-20^\circ\text{C}$ . Both detectors have 100 ms temporal resolution characteristics, which make them most appropriate for solar flare research in the context of energy transport and acceleration time scales of particles.

The instrumentation of the SLD payload, its in-flight calibration and operation has been described by Jain *et al.* (2005, 2006a). The SLD payload is functioning

**Table 1.** Physical characteristics of SLD/SOXS flares considered for current investigation.

Sl. no.	Date	Begin	Time UT		Peak Int. <sup>a</sup>	GOES Class	Active Region	
			Peak	End			Location	NOAA
1.	30 Jul 03	04:07	04:09	04:28	5700	M2.5	N16 W25	10422
2.	19 Nov 03	04:54	05:01	05:10	2660	M1.7	N01 E06	10501
3.	07 Jan 04	<03:55	04:00	04:33	5470	M4.5	N02 E82	10537
4.	25 Mar 04	04:29	04:38	05:07	4180	M2.3	N12 E82	10582
5.	25 Apr 04	05:28	05:36	05:58	4900	M2.2	N13 E38	10599
6.	14 Jul 04	05:18	05:23	>05:25	10750	M6.2	N12 W62	10646
7.	14 Aug 04	05:37	05:44	>06:04	18630	M7.4	S11 W28	10656
8.	31 Oct 04	05:26	05:31	05:46	4830	M2.3	N13 W34	10691
9.	15 Jan 05	04:28	04:31	04:52	10260	M8.4	N14 E06	10720
10.	27 Jul 05	04:34	04:58	>05:30	5800	M3.7	N08 E88	10792
11.	03 Aug 05	04:57	05:05	05:19	5350	M3.4	S11 E36	10794
12.	25 Aug 05	04:36	04:39	04:52	11140	M6.4	N07 E78	10803
13.	09 Sep 05	05:25	05:48	06:17	10800	M6.2	S10 E66	10808
14.	17 Sep 05	06:00	06:05	>06:20	13170	M9.8	S12 W40	10808

**Note** :>After; <: Before, <sup>a</sup>Peak intensity in 4.1–24.5 keV in counts/second.

satisfactorily onboard the GSAT-2 spacecraft since its launch on 8 May 2003, and so far more than 700 important flares greater than *GOES* class B3.0 have been observed. The spectral resolution revealed by Si detector is 0.7 keV @ 6 keV and 0.8 keV @ 22.2 keV, which is better than the earlier detectors used for solar flare research in this energy range. Further, its temporal resolution is 100 ms during flare mode in order to achieve feasible energy spectrum. The SLD provides data in temporal and spectral modes.

## 2.2 Dataset

We selected a total 14 flares of *GOES* importance class M (Table 1) observed by Si detector for the current investigation. The flare temporal characteristics are shown in this table. The table also gives the peak intensity measured in 4.1–24.5 keV energy band. The active region number and flare location have been obtained from Solar & Geophysical Data (SGD) reports. In addition to temporal data, the experiment provides spectral mode observations in the energy range of 4–25 keV with a channel resolution of 0.082 keV.

## 2.3 Temporal evolution

In Fig. 1, we show the temporal evolution of the 25 August 2005 flare in four different energy bands using spectral data of the Si detector. The time resolution for spectral mode observations during the quiet period is 3 s but during flare mode it is 100 ms, which however, is restricted to 287.5 s only in view of telemetry constraints. The light curves (intensity as a function of time) are shown in  $\sim$ 4.1–10, 10–15, 15–20 and 20–25 keV energy bands. The flare starts around 04:36 UT and peaks around 04:39 UT whereas it ends around 04:52 UT in 4.1–24.5 keV energy band (Table 1). It may also be noted from Fig. 1 that the 25 August 2005 flare peaks faster through the quick reconnection process and also decays faster compared to many other flares (Table 1).

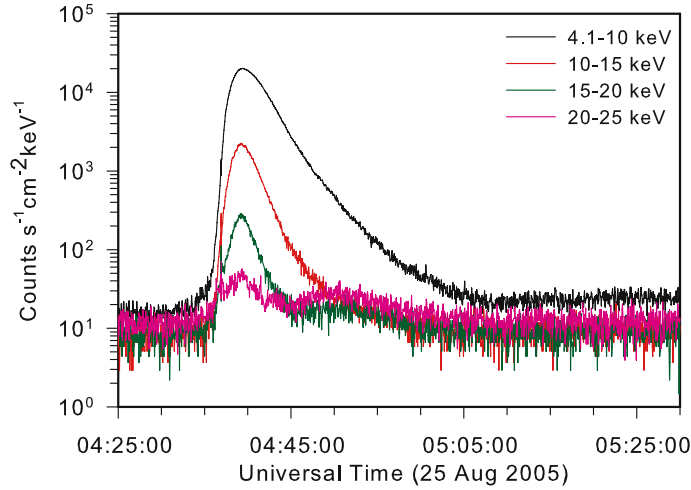


**Figure 1.** Light curves of the 25 August 2005 solar flare as recorded by Si detector of SLD/SOXS mission.

The onset of flare is delayed in higher and higher energy channels but peaks earlier in higher energy bands. This suggests that the higher energy 15–25 keV X-ray photons are produced by thermal emission of higher temperature, i.e., 10–40 MK which have a shorter thermal conduction time than the lower energy channels 4–15 keV which contain thermal emission of lower temperature (Jain *et al.* 2010).

#### 2.4 Spectral evolution

The spectral evolution of the 25 August 2005 flare is shown in Fig. 2. The low intensity below 6 keV is due to aluminum plus kapton filter mounted on the detector head to cut the X-ray photons up to 4 keV and electrons up to 300 keV falling in the line-of-sight of the detector. It may be noted that the Fe and Fe–Ni lines are unambiguously visible in the count spectra at  $\sim 6.7$  and  $\sim 8$  keV, respectively, however, their intensity and width vary over time. The count spectra are de-convoluted over the instrumental response to obtain the photon spectra. The pre-flare background has been subtracted from the observed counts during flare time as shown in Data-Bk in Fig. 2. The Fe-line feature is observed during the whole flare while visibility of Fe–Ni feature is only for short intervals depending on the suitability of temperature required for its formation.

We use the OSPEX (Object Spectral Executive) software package inside SolarSoft to analyze the Si detector spectra. The OSPEX is an object-oriented interface for X-ray spectral analysis of solar data. It is the next generation of SPEX (Spectral Executive) written by R. Schwartz in 1995. Through OSPEX, the user reads and displays the input data, selects and subtracts background, selects time intervals of interest, selects a combination of photon flux model components to describe the data, and fits those components to the spectrum in each selected time interval. The SLD instrumental response is incorporated in SolarSoft to enable analyzing data world-wide. During the fitting process, the response matrix is used to convert the photon model to model counts to compare with the input count data. The resulting time-ordered fit parameters are

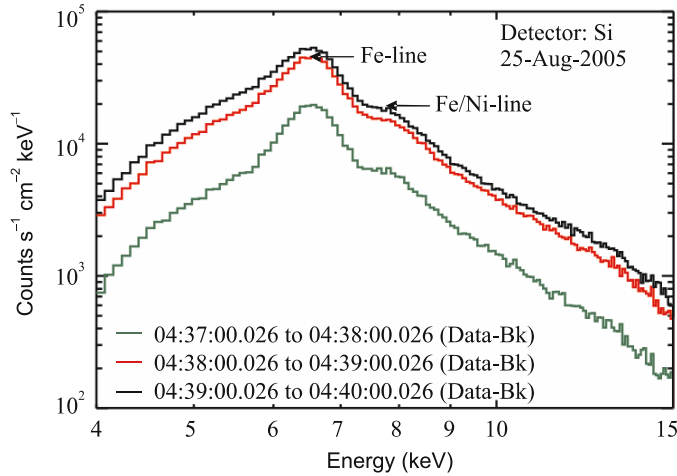


**Figure 2.** Spectra of the 25 August 2005 solar flare in the energy bands 4–15 keV at three different time intervals showing evolution of Fe and Fe–Ni line features.

stored and can be displayed and analyzed with OSPEX. The entire OSPEX session can be saved in the form of a script and the fit results stored in the form of a FITS file.

The OSPEX subroutines have been updated to undertake detailed temporal and spectral data analysis of Si and CZT detectors of SLD/SOXS mission. The raw data for spectral mode observations is first checked for any spurious or false flare as well as for pre-flare background. The spectrum at a given time is made by integrating the spectra over an interval of 30–60 s. OSPEX enables us to look at the temporal evolution, spectrogram and spectral evolution. It also enables us to fit energy spectra using Chianti codes (Dere *et al.* 1997). We employed Chianti 5.2 version for current investigation (Landi *et al.* 2006) of flare plasma diagnostics with the application of line emission, multi-thermal, and non-thermal functions.

### 3. Results and discussion

In order to study the Fe and Fe–Ni line emission it is more important to study their evolution with the flare development, i.e., as a function of temperature because the line emission and its intensity vary with temperature and emission measure (Phillips 2004). It may be noted from Fig. 2 that the peak intensity, peak energy and area under the curve of the lines vary over time. In fact, the plasma temperature and hence emission measure vary over time and these factors mainly control the shape of the line. The non-thermal contribution also plays a role and therefore needs to be considered as an important parameter including temperature and emission measure.

The Fe-line feature is here defined as the excess above the continuum, as observed by Si spectrometer with spectral resolution (FWHM)  $\leq 0.8$  keV, in the energy range 5.8–7.5 keV, and similarly the Fe–Ni line feature in the range 7.5–9.2 keV (Phillips 2004). We analyzed 10–23 spectra, for each flare under study, depending on the duration of the flare. A total of 250 spectra of 14 flare events listed in Table 1 have been analyzed and considered for spectral fit. We use forward fitting program in OSPEX to fit the count spectra. The important aspect of our spectra-fit analysis is the consideration

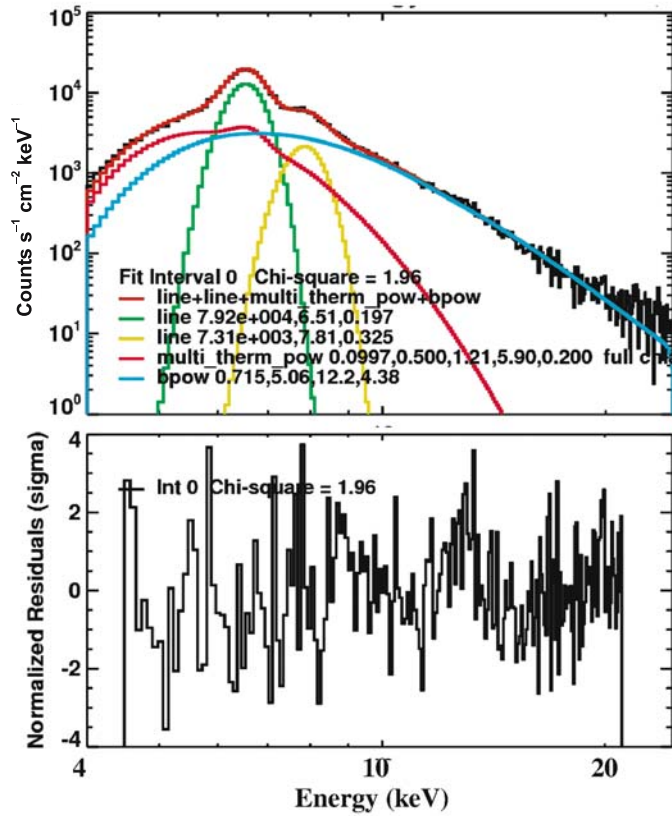


**Figure 3.** Fit count spectra of the 25 August 2005 flare considering line Gaussian, multi-thermal and broken power-law functions using Chianti codes. Residuals as a function of energy for the fit count spectra are shown in the lower panel. Derived plasma fit parameters are shown on the count spectra.

of multi-thermal power-law function (Jain *et al.* 2008), which assumes differential emission measure (DEM) in addition to line emission and broken power-law functions. Analysis techniques considering these functions have been recently described in detail by Jain *et al.* (2008). The DEM analysis on the 2003 February 22 RESIK flare was carried out by Chifor *et al.* (2007) which describes the multi-thermal nature of the emitting plasma, confirming the presence of a dominant temperature component, peaking close to the temperatures at which the RESIK line and continuum *EM* curves intersect. More recently, Aschwanden (2008) proposed multi-thermal diagnostics of Fe and Fe–Ni-line complex and conduction cooling delays in flare plasma.

In Fig. 3, we show a typical example of count spectra-fit with application of the above functions. The line Gaussian function allows measuring of the integrated intensity and centroid energy of Fe and Fe–Ni line features. The multi-thermal power-law function enables measuring of the minimum and maximum temperature of the flare plasma, power-law index and the flux of Fe-line and Fe–Ni-line features relative to corona. However, the minimum coronal plasma temperature is considered to be constant = 0.5 keV, while the maximum plasma temperature is a free parameter and determined by best-fit. The broken power-law considers continuum X-ray emission

from thermal and non-thermal bremsstrahlung distribution, and reveals power-law index below and above break energy. The Si detector allows fitting of the spectrum with an uncertainty of  $\pm 1$  channel corresponding to error in temperature measurements of  $\pm 0.95$  MK.

The energy range to fit the whole spectrum was considered between 4.1 keV and  $\sim 23$  keV, depending on the signal-to-noise characteristics of the spectrum. In order to obtain the relative flux of Fe to Fe–Ni-line features we divide the integrated intensity flux of Fe-line features by the integrated intensity flux of Fe–Ni-line features. Therefore, in the spectra fitting process the integrated intensity is kept free to vary during the fitting process while the peak energy and line width were varied manually to get reduced chi-squared ( $\chi^2$ ) values minimum. The residual (i.e., standard deviation of the theoretical model count above or below the experimental count in each energy bin) in the fit range is also obtained as shown in the bottom of the fitted spectrum of the 25 August 2005 during 04:37 to 04:38 UT in Fig. 3. The error in each fit parameter is obtained after fitting the whole spectra by line (Fe-line)–line (Fe–Ni line), multi-thermal and broken power-law to the experimental data of count spectra.

The error in the measured flux of Fe and Fe–Ni line is used to obtain the relative error. Here the error in relative flux of Fe to Fe–Ni,  $\Delta(\text{Fe}/\text{Ni})$ , is obtained by the following formula:

$$\Delta\left(\frac{\text{Fe}}{\text{Ni}}\right) = \frac{\text{Fe}}{\text{Ni}} \sqrt{\left[\left(\frac{\Delta\text{Fe}}{\text{Fe}}\right)^2 + \left(\frac{\Delta\text{Ni}}{\text{Ni}}\right)^2\right]}, \quad (1)$$

where  $\Delta\text{Fe}$  and  $\Delta\text{Ni}$  are the errors in Fe and Fe–Ni line fluxes, respectively.

The measured error bars in Fe to Fe–Ni flux ratio are shown in the y-axis of Fig. 4.

In Fig. 4, we show the intensity ratio of Fe-line to Fe–Ni-line features as a function of electron plasma temperature measured for all flares. The intensity of Fe-line and

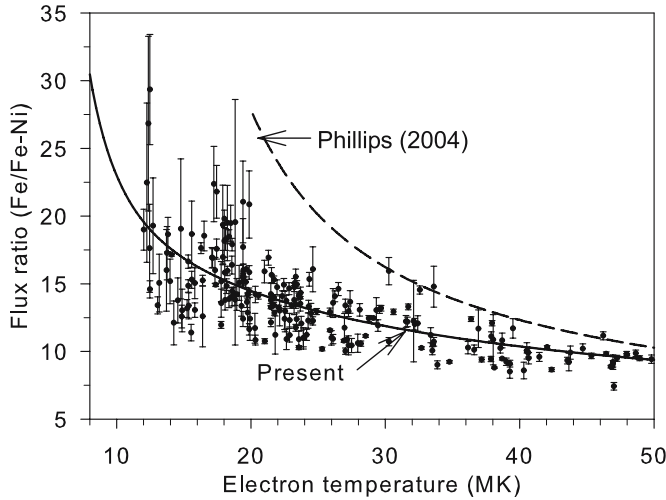


**Figure 4.** Variation of flux ratio of Fe-line to Fe–Ni-line features relative to coronal flux as a function of electron temperature in X-ray flares. The error bars shown in the x-axis represent uncertainty in temperature measurements of  $\pm 0.95$  MK. The y-axis error has been measured from line feature intensity measurements (see text).

Fe–Ni-line features gives a direct measure of their respective fluxes relative to coronal flux, and the ratio of their intensity is, therefore, a measure of the relative flux of these two line features relative to coronal flux. It may be noted from Fig. 4 that the relative flux drops drastically from  $\sim 30$  at 12 MK to  $\sim 15$  at 20 MK, and then decays slowly with temperature. The solid line showing the best fit to the data is presented by the asymptotic form of polynomial of inverse third order as follows:

$$y = y_0 + \left(\frac{a}{x}\right) + \left(\frac{b}{x^2}\right) + \left(\frac{c}{x^3}\right), \quad (2)$$

where the parameters are as follows:

$$\begin{aligned} y_0 &= 4.3511, & a &= 299.6151, \\ b &= -2754.9715, & c &= 16222.3405. \end{aligned}$$

The relative flux ratio is  $\sim 30$  at temperature  $\sim 12$  MK which drops to half  $\sim 15$  at 20 MK, and at further higher temperatures it decreases smoothly reaching to  $\sim 8$  at 50 MK. However, the theoretically expected flux ratio from Phillips (2004), shown in Fig. 4 (dashed line) is very high relative to that measured by us in this investigation. This may be due to the consideration of higher values of Fe and Fe–Ni line densities in his model.

#### 4. Conclusions

Phillips *et al.* (2004) and Jain *et al.* (2006b) showed that the observed equivalent widths ( $w$ ) of Fe-line increase with  $T_e$  more sharply than what is predicted by the theoretical curve, with a clear displacement to higher temperatures being indicated. These results are not so easily explained. If the isothermal approximation is a good one for spectra during these flares, as is indicated by the reduced  $\chi^2$  values, then possibly this behaviour could indicate the need for a correction to the ionization fractions of Mazzotta *et al.* (1998). This points to differential emission measure indicating to multi-temperature model instead of single temperature approximation that was considered so far in the X-ray spectral analysis of the flares.

We conclude that our analysis assuming line Gaussian, multi-thermal and broken power-law to fit the spectra of solar flares observed by Si detector of SLD/SOXS mission may improve the diagnostics of flare plasma. Particularly, application of the above functions in fitting the X-ray spectra of solar flares allowed us to measure the flux ratio of Fe-line to Fe–Ni-line features relative to coronal flux which varies with electron temperature as an inverse polynomial in agreement to theoretically predicted by Phillips (2004). However, comparison of the present measurements with the theoretical predictions of Phillips (2004) suggests revising the Fe and Fe–Ni line densities in the corona.

#### Acknowledgements

The authors express their sincere thanks to Prof. Brian R. Dennis, Dr. Richard Schwartz and Ms. Kim Tolbert (GSFC, Washington) for their valuable advice on the interpretation of the spectral analysis, and for developing the software which enabled analyzing the SOXS data. The authors also express their sincere gratitude to Prof. K. J. H. Phillips (MSSL, UK) for valuable advice during this investigation.

## References

- Aschwanden, M. J. 2008, *J. Astrophys. Astron.*, **29**, 3.
- Chifor, C., Del Zanna, G., Mason, H. E., Sylwester, J., Sylwester, B., Phillips, K. J. H. 2007, *Astron. Astrophys.*, **462**, 323.
- Dennis, B. R., Phillips, K. J. H., Sylwester, J., Sylwester, B., Schwartz, R. A., Tolbert, A. K. 2005, *Adv. Space Res.*, **35**, 1723.
- Dere, K. P., Landi, E., Mason, H. E., Monsignori Fossi, B. C., Young, P. R. 1997, *A&A Suppl. Ser.*, **125**, 149.
- Jain, Rajmal, Rao, A. R., Deshpande, M. R., Dwivedi, B. N., Manoharan, P. K., Seetha, S., Vahia, M. N., Vats, H. O., Venkatkrishnan, P. 2000a, *Bull. Astron. Soc. India*, **29**, 117.
- Jain, Rajmal, Deshpande, M. R., Dave, H. H., Manian, K. S. B., Vadher, N. M., Shah, A. B., Ubale, G. P., Mecwan, G. A., Trivedi, J. M., Solanki, C. M., Shah, V. M., Patel, V. D., Kayasth, S. L., Sharma, M. R., Umopathy, C. N., Kulkarni, R., Kumar, Jain, A. K., Sreekumar, P. 2000b, Technical Document – *GSAT-2 Spacecraft – Preliminary Design Review (PDR) Document for Solar X-ray Spectrometer*, **ISRO-ISAC-GSAT-2-RR-0155**.
- Jain, Rajmal, Dave, H. H., Shah, A. B., Vadher, N. M., Shah, V. M., Ubale, G. P., Manian, K. S. B., Solanki, C. M., Shah, K. J., Kumar, Sumit, Kayasth, S. L., Patel, V. D., Trivedi, J. J., Deshpande, M. R. 2005, *Solar Phys.*, **227**, 89.
- Jain, Rajmal, Joshi Vishal, Kayasth, S. L., Dave, Hemant, Deshpande, M. R. 2006a, *J. Astrophys. Astron.*, **27**, 175.
- Jain, Rajmal, Pradhan, A. K., Joshi, Vishal, Shah, K. J., Trivedi, Jayshree J., Kayasth, S. L., Shah, Vishal M., Deshpande, M. R. 2006b, *Solar Phys.*, **239(1–2)**, 217.
- Jain, Rajmal, Aggarwal, Malini, Sharma, Raghunandan 2008, *J. Astrophys. Astron.*, **29**, 125.
- Jain, Rajmal, Rajpurohit, A. S., Aggarwal, M., Jamwal, R., Awasthi, A. 2010, Magnetic Coupling between the Interior and Atmosphere of the Sun (eds) Hasan, S. S., Rutten, R. J.; *Astrophysics and Space Science Proceedings*. ISSN 1570–6591 (Print), pp. 465–470.
- Landi, E., Del Zanna, G., Young, P. R., Dere, K. P., Mason, H. E., Landini, M. 2006, *ApJS*, **162(1)**, 261.
- Mazzotta, P., Mazzitelli, G., Colafrancesco, S., Vittorio, N. 1998, *A&A. Suppl.*, **133**, 403.
- Phillips, K. J. H. 2004, *ApJ*, **605**, 921.
- Phillips, K. J. H., Dennis, B. R., Sylwester, J., Sylwester, B. 2004, American Astronomical Society Meeting 204, *Bull. Amer. Astron. Soc.*, **36**, 818.